

Semiclassical multi-phonon theory for atom-surface scattering: Application to the Cu(111) system

Shauli Daon and Eli Pollak

Citation: *The Journal of Chemical Physics* **142**, 174102 (2015); doi: 10.1063/1.4919345

View online: <http://dx.doi.org/10.1063/1.4919345>

View Table of Contents: <http://scitation.aip.org/content/aip/journal/jcp/142/17?ver=pdfcov>

Published by the AIP Publishing

Articles you may be interested in

[Spectral phonon conduction and dominant scattering pathways in graphene](#)

J. Appl. Phys. **110**, 094312 (2011); 10.1063/1.3656451

[Classical theory for the in-plane scattering of atoms from corrugated surfaces: Application to the Ar-Ag\(111\) system](#)

J. Chem. Phys. **130**, 194710 (2009); 10.1063/1.3131182

[Erratum: "Molecular dynamics study of vibrational energy relaxation of CN – in H₂O and D₂O solutions: An application of path integral influence functional theory to multiphonon processes" \[*J. Chem. Phys.* 111, 5390 \(1999\)\]](#)

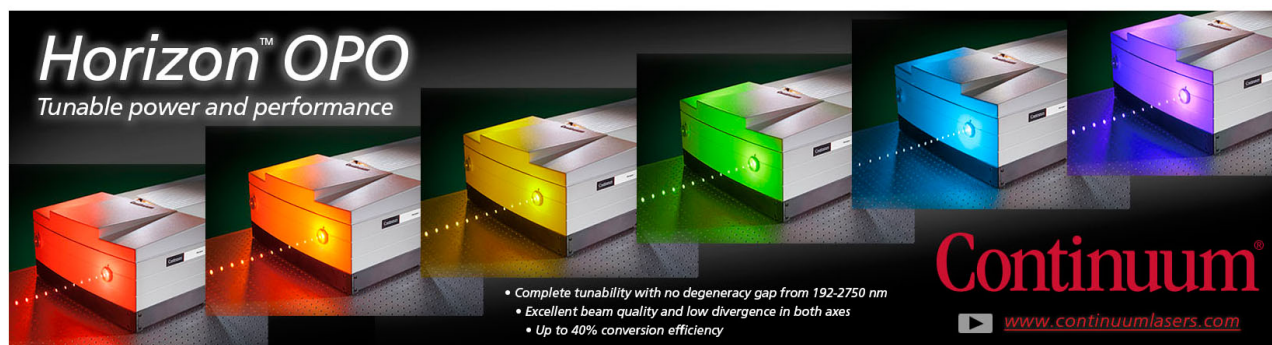
J. Chem. Phys. **113**, 6451 (2000); 10.1063/1.1308088

[Multiphonon He atom scattering from Xe overlayers on Cu\(111\) and Cu\(001\) surfaces](#)

J. Chem. Phys. **106**, 9922 (1997); 10.1063/1.473839

[The transition from single phonon to multiphonon energy transfer in atom-surface collisions](#)

J. Chem. Phys. **106**, 1234 (1997); 10.1063/1.473220



Horizon™ OPO
Tunable power and performance

- Complete tunability with no degeneracy gap from 192-2750 nm
- Excellent beam quality and low divergence in both axes
- Up to 40% conversion efficiency

Continuum®
www.continuumlasers.com

Semiclassical multi-phonon theory for atom-surface scattering: Application to the Cu(111) system

Shauli Daon and Eli Pollak

Chemical Physics Department, Weizmann Institute of Science, 76100 Rehovoth, Israel

(Received 6 March 2015; accepted 17 April 2015; published online 1 May 2015)

The semiclassical perturbation theory of Hubbard and Miller [J. Chem. Phys. **80**, 5827 (1984)] is further developed to include the full multi-phonon transitions in atom-surface scattering. A practically applicable expression is developed for the angular scattering distribution by utilising a discretized bath of oscillators, instead of the continuum limit. At sufficiently low surface temperature good agreement is found between the present multi-phonon theory and the previous one-, and two-phonon theory derived in the continuum limit in our previous study [Daon, Pollak, and Miret-Artés, J. Chem. Phys. **137**, 201103 (2012)]. The theory is applied to the measured angular distributions of Ne, Ar, and Kr scattered from a Cu(111) surface. We find that the present multi-phonon theory substantially improves the agreement between experiment and theory, especially at the higher surface temperatures. This provides evidence for the importance of multi-phonon transitions in determining the angular distribution as the surface temperature is increased. © 2015 AIP Publishing LLC. [<http://dx.doi.org/10.1063/1.4919345>]

I. INTRODUCTION

The first observations of quantum diffraction of He scattered from a LiF surface were reported 80 years ago.^{1,2} Since then, many authors repeated such experiments with increasing sophistication.³ It is well understood that diffraction peaks found in surface scattering of atoms as heavy as Kr are due to the periodic corrugation of the surface.

The quantum theory of scattering from surfaces has been developed extensively. Manson and coworkers used a Distorted Wave Born Approximation (DWBA) approach.^{4–6} A semiclassical theory of atom-surface scattering was proposed by Billing.^{7,8} The surface was treated as a set of coupled quantum oscillators perturbed by the time-dependent force imposed by the colliding atom/molecule. Miret-Artés and others used a quantum trajectory-based formalism to describe quantum mechanical phenomena such as selective adsorption^{9,10} and quantum close-coupling calculations to describe the He surface interaction potential for scattering on Sb(111) and ZnO surfaces.^{11–13} Jackson used a time-dependent mean-field approach¹⁴ and wavepacket propagation methods¹⁵ in a restricted two-dimensional model to simulate the underlying quantum dynamics. Gumhalter and co-workers developed an evolution operator theory and applied it to atom-surface scattering.^{16–18} Gross used reduced-dimensional quantum mechanics simulations¹⁹ along with a potential obtained using density functional theory to study the scattering of hydrogen molecules from a Pd(100) surface.²⁰ Nieto *et al.*,²¹ using a combination of quantum scattering theory and experiment, showed that the scattering of H₂ from a metal surface occurs on a single Born-Oppenheimer potential energy surface. Three dimensional semiclassical studies of atom surface scattering were carried out by Drolshagen and Heller, employing a thawed Gaussian wavepacket method giving good agreement with numerically exact quantum mechanical results.²²

The classical theory of atom surface scattering has also been developed.²³ The double lobe structure found in many measurements of the angular distribution of the scattered particle was attributed to classical rainbows. The study of model hard wall corrugated potentials has shown that for weak corrugation, one should expect that at the inflection points of the corrugation, the derivative of the angular deflection function vanishes, leading to a divergence of the scattering probability. Smearing of this divergence due to thermal fluctuations then leads to the double lobe structure. The earliest models considered a hard wall corrugated potential for which one can solve the scattering analytically.^{24–30} Adding a potential well in front of the hard wall accounted for the energy dependence of the angular distance between the rainbow peaks. As the energy is increased, the refraction caused by the potential well decreases, and the rainbow angles come closer to each other. This class of models was then improved to include thermal effects, by treating the surface as a particle with an effective mass and thermally distributed velocity, and is known as the washboard model.²⁶

In recent years, the classical theory has been further developed to include more realistic “soft” potentials and a harmonic continuum description of surface phonons.^{31–35} Noting that both the corrugation height and the friction felt by the incoming particle are typically small, one can solve for the classical dynamics using a classical perturbation theory. This accounts well for many of the qualitative features of the angular distributions, including the dependence on incident energy, incident angle, surface temperature, and more. If one models the interaction potential in terms of a Morse potential and sinusoidal corrugations along the horizontal surface directions, one can derive an analytic theory for the scattering. This approach was then used to invert the measured angular distributions in terms of interaction potentials. Very recently, the perturbation theory has been expanded to include the second order corrections due to the surface corrugation.³⁶

In this paper, we follow a semiclassical route, pioneered by Miller and coworkers. Using SemiClassical Perturbation Theory (SCPT),³⁷ Hubbard and Miller derived^{38,39} simple expressions, in terms of integer Bessel functions for the elastic scattering of an atom from a frozen surface. They, then, also considered thermal effects³⁹ albeit in a limited manner, considering an Einstein phonon spectrum.

Notwithstanding these developments, there remain many experimental features, associated with the quantum scattering of heavy atoms on surfaces which have yet to receive a satisfactory explanation. Andersson and co-workers^{40,41} studied in some detail the scattering of Ne, Ar, and Kr on a Cu(111) surface. Using very cold surfaces and low energy beams, they were able to observe diffraction peaks in the angular distribution even for an atom as heavy as Kr. They also observed a relatively smooth “background” angular scattering. A theory which correctly accounts for both the diffraction peaks and the smooth background as well as their temperature dependence is the central objective of this paper. In a previous Communication,⁴² we noted that the broad background may be inverted to determine the phonon spectral density. However, our previous analysis was restricted to only single and two phonon transitions and so did not provide a complete description of the thermal effects.

The theory we use is an extension of the SCPT of Hubbard and Miller.³⁹ Our starting point is a Hamiltonian description of the scattering in which the particle is coupled linearly to a bath of harmonic oscillators, whose properties are described by a continuum spectral density. Systematic application of SCPT enables us to derive a practical theory which includes realistic force fields as well as thermal effects of the surface.

The SCPT approach is based on the observation that often, especially when scattering from metal surfaces, the corrugation of the surface is weak so that the corrugation height may be considered as a small parameter justifying a perturbative solution of the equations of motion. Similarly, the coupling to the phonons is weak so that this coupling too may be considered within perturbation theory.

In contrast, though, to previous work, we introduce here a form factor which enables the computation of the angular distribution with an arbitrary number of phonon transitions. The resulting multi-phonon theory, which uses a discretization of the spectral density, is then applied to a study of the scattering of Ne, Ar, and Kr on a Cu(100) surface, as measured by Andersson and coworkers.^{40,41}

The semiclassical theory is developed in Sec. II. It is applied in Sec. III to the experimental results of Andersson and coworkers^{40,41} for the scattering of Ne, Ar, and Kr from the Cu(100) surface. We end with a discussion of the limitations and further possible extensions of the semiclassical theory.

II. SEMICLASSICAL PERTURBATION THEORY

A. The framework

Since the typical experimental measurements are carried out in the plane of the incident and outgoing beams, we will

restrict ourselves here and model the dynamics in terms of two degrees of freedom. One is the vertical distance z (with conjugate momentum p_z) describing the distance of the atom (whose mass is M) from the surface, the other is the horizontal coordinate x (with conjugate momentum p_x) parallel to the surface. Recent classical studies have shown⁴³ that the two planar degrees of freedom (x and y) are not necessarily separable so that inclusion of the second planar degree of freedom can change the classical scattering dynamics. It should be thus understood that the present treatment is valid provided that the coupling between the two degrees of freedom may be neglected. Furthermore, we will assume that the coupling to the vertical phonons is much more important than the coupling to the horizontal surface phonons. This assumption has also been verified in recent on the fly molecular dynamics computations.⁴³

The model Hamiltonian we use is based on the assumption that the interaction of the particle with the surface is only dependent on the instantaneous distance of the particle from the fluctuating surface which is $z + h(x) + \frac{1}{\sqrt{M}} \sum_{j=1}^N c_j x_j$. The fluctuational part is assumed small so that to leading order in the coupling, the potential of interaction is a sum of three terms $\bar{V}(z + h(x) + \frac{1}{\sqrt{M}} \sum_{j=1}^N c_j x_j) \simeq \bar{V}(z) + \bar{V}'(\hat{z})h(\hat{x}) + \bar{V}'(\hat{z})\frac{1}{\sqrt{M}} \sum_{j=1}^N c_j x_j$. The resulting “standard” model Hamiltonian^{23,42} describing the scattering dynamics is

$$\hat{H} = \frac{\hat{p}_x^2 + \hat{p}_z^2}{2M} + \bar{V}(\hat{z}) + \bar{V}'(\hat{z})h(\hat{x}) + \sum_{j=1}^N \left[\frac{\hat{p}_j^2}{2} + \frac{\omega_j^2}{2} \left(\hat{x}_j - \frac{c_j \bar{V}'(\hat{z})}{\sqrt{M}\omega_j^2} \right)^2 \right], \quad (2.1)$$

where $\bar{V}(\hat{z})$ is the potential of interaction in the vertical direction; $\bar{V}'(\hat{z})$ denotes the derivative of the potential $\bar{V}(\hat{z})$ with respect to z ; $h(\hat{x})$ is the horizontal corrugation function which in this paper will take the simple form

$$h(\hat{x}) = h \sin \left(\frac{2\pi \hat{x}}{l} \right), \quad (2.2)$$

where h is the corrugation height parameter, considered to be small compared to the lattice length l of the surface in the horizontal direction, \hat{p}_j and \hat{x}_j are the respective mass weighted momentum and coordinate operators for the j -th bath oscillator, and c_j is the dimensionless coupling constant which couples the j -th bath oscillator to the vertical motion.

The continuum limit is introduced through the spectral density defined as

$$J_z(\omega) = \frac{\pi}{2} \sum_{j=1}^N \frac{c_j^2}{\omega_j} \delta(\omega - \omega_j). \quad (2.3)$$

The associated friction function is

$$\gamma(t) = \sum_{j=1}^N \frac{c_j^2}{\omega_j^2} \cos(\omega_j t). \quad (2.4)$$

In this paper, we concentrate on the angular distribution of the scattered particle initiated far away from the surface at the time $-t_0$ with initial (negative) momentum p_{z_i} and (positive) horizontal momentum p_{x_i} . We are then interested in the

distribution of the final momenta p_{zf} and p_{xf} of the particle at the time $+t_0$, which is taken to be sufficiently large to assure that the scattering event is over. The initial state of the system is also characterized by the initial quantum number n_{ji} of the j -th bath oscillator and the final quantum state n_{jf} of the j -th oscillator after the collision is over.

The periodicity of the surface in the horizontal direction implies that the final momentum must obey the Bragg condition, that is,

$$p_{xf} = p_{xi} + \frac{2\pi\hbar n}{l}, \quad (2.5)$$

with n an integer and referred to as the Bragg number. Energy conservation then implies that the vertical momentum of the particle, after the collision is over, p_{zt_0} , is related to all other observables through the energy conservation relationship

$$\begin{aligned} \frac{p_{zt_0}^2 + (p_{xi} + \frac{2\pi\hbar n}{l})^2}{2M} + \sum_{j=1}^N \left(n_{jf} + \frac{1}{2} \right) \hbar\omega_j \\ = \frac{p_{zi}^2 + p_{xi}^2}{2M} + \sum_{j=1}^N \left(n_{ji} + \frac{1}{2} \right) \hbar\omega_j. \end{aligned} \quad (2.6)$$

The exact quantum mechanical final particle momentum distribution, summed over all possible final bath states, is then by definition

$$\begin{aligned} P(p_{xf}, p_{zf}; \mathbf{n}_i) = \sum_{n, n_f} \delta(p_{xf} - p_{xi} - \frac{2\pi\hbar n}{l}) \\ \times \delta(p_{zf} - p_{zi}) P_{n, n_f; 0, n_i}, \end{aligned} \quad (2.7)$$

where the vector notation $\mathbf{n} = (n_1, \dots, n_N)$ is used to describe all the bath mode quantum numbers. $P_{n, n_f; 0, n_i}$ is the quantum probability for going from the initial state of the bath (\mathbf{n}_i) and the initial momenta of the particle (p_{xi}, p_{zi} with Bragg number $n_i = 0$ by definition) to the respective final momenta and oscillator quantum states. For future use, we note that the change in the occupation numbers of the oscillators is defined as

$$\Delta \mathbf{n} = \mathbf{n}_f - \mathbf{n}_i. \quad (2.8)$$

The heart of the theory is the diffraction probability

$$P_{n, n_f; 0, n_i} = |S_{n, n_f; 0, n_i}|^2, \quad (2.9)$$

where $S_{n, n_f; 0, n_i}$ is the corresponding S-matrix element.

Typically, the surface is in thermal equilibrium with temperature T , so that the initial condition for the bath is described by the thermal bath density operator

$$\hat{P}_B = \frac{\exp(-\beta \hat{H}_B)}{Z_B}, \quad (2.10)$$

where $Z_B = \text{Tr}_B \exp(-\beta \hat{H}_B)$ is the bath partition function and the bath Hamiltonian is defined as

$$\hat{H}_B = \sum_{j=1}^N \left[\frac{\hat{p}_j^2}{2} + \frac{\omega_j^2}{2} \hat{x}_j^2 \right] \quad (2.11)$$

and $\beta = 1/(k_B T)$. The thermally averaged final momentum distribution is then

$$\begin{aligned} \langle P(p_{xf}, p_{zf}) \rangle_\beta = \sum_{n_i=0}^{\infty} \sum_{n, n_f} \delta(p_{xf} - p_{xi} - \frac{2\pi\hbar n}{l}) \delta(p_{zf} - p_{zi}) \\ \cdot P_{n, n_f; 0, n_i} \frac{\exp(-\beta \hbar ((\mathbf{n}_i + \frac{1}{2} \mathbf{I}) \cdot \boldsymbol{\omega}))}{Z_B}. \end{aligned} \quad (2.12)$$

The (negative) angle of incidence θ_i and the final scattering angle θ_f relative to the normal to the surface are by definition

$$\theta_j = \tan^{-1} \left(\frac{p_{xj}}{p_{zj}} \right), \quad j = i, f. \quad (2.13)$$

The thermally averaged final angular distribution of the scattered particle is then given in terms of the final momentum distribution as

$$\begin{aligned} \langle P(\theta_f) \rangle_\beta = \int_{-\infty}^{\infty} dp_{xf} \int_0^{\infty} dp_{zf} \delta \left(\theta_f - \tan^{-1} \left(\frac{p_{xf}}{p_{zf}} \right) \right) \\ \times \langle P(p_{xf}, p_{zf}) \rangle_\beta. \end{aligned} \quad (2.14)$$

B. Semiclassical theory

Forty-five years ago, Miller^{44,45} formulated an initial value representation for the S-matrix element. To introduce his expression, we first define the classical action angle variables for the system and the bath. The system angle variable q_x is defined in terms of the horizontal coordinate of the particle and the lattice length of the surface as

$$q_x = \frac{2\pi x}{l}. \quad (2.15)$$

The corresponding horizontal action variable is defined as

$$I_x = \frac{l p_x}{2\pi}. \quad (2.16)$$

The bath action (I_j) and angle (q_j) variables for the j -th bath oscillator are defined by the canonical transformation

$$x_j = \sqrt{\frac{2I_j}{\omega_j}} \cos(q_j), \quad (2.17)$$

$$p_j = -\sqrt{2\omega_j I_j} \sin(q_j). \quad (2.18)$$

The initial conditions for the classical actions are

$$I_{ji} = \hbar \left(n_{ji} + \frac{1}{2} \right), \quad j = 1, \dots, N. \quad (2.19)$$

To get rid of infinities at long times after the collision, Miller also introduced the pseudo angle variables

$$\bar{q}_{jt} = q_{jt} - \frac{M z_t \omega_j}{p_{zt}}, \quad j = 1, \dots, N \quad (2.20)$$

such that at long times after the classical collision is over, when the particle is moving freely, one has that for the j -th oscillator $\frac{d\bar{q}_{jt}}{dt} = 0$. Similarly one introduces a pseudo angle variable for the horizontal motion

$$\bar{q}_{xt} = q_{xt} - \frac{M z_t \omega_x}{p_{zt}}, \quad (2.21)$$

where the horizontal frequency is defined as

$$\omega_{x_t} = \frac{2\pi p_{x_t}}{Ml}. \quad (2.22)$$

Miller derived the following initial value representation for the classical S-matrix element:⁴⁵

$$S_{n_{x_f}, n_f; 0, n_i} = \lim_{t_0 \rightarrow \infty} \int_0^{2\pi} \frac{dq_{x_i}}{2\pi} \int_0^{2\pi} \prod_{j=1}^N \frac{dq_{j_i}}{2\pi} |\mathbf{D}|^{1/2} \cdot \exp \left(\frac{i}{\hbar} \left[\varphi_{t_0} + \bar{q}_{x_{t_0}} (I_{x_{t_0}} - \hbar n_{x_f}) + \sum_{j=1}^N \bar{q}_{j_{t_0}} \left(I_{j_{t_0}} - \hbar \left(n_{j_f} + \frac{1}{2} \right) \right) \right] \right), \quad (2.23)$$

where $I_{x_{t_0}}$, $\bar{q}_{x_{t_0}}$ and $I_{j_{t_0}}$, $\bar{q}_{j_{t_0}}$, $j = 1, \dots, N$ are the values of the respective action and pseudo angle variables, after the collision is over. The action is

$$\varphi_{t_0} = - \int_{-t_0}^{t_0} dt [q_{x_t} \dot{I}_{x_t} + z_t \dot{p}_{z_t} + \sum_{j=1}^N q_{j_t} \dot{I}_{j_t}]. \quad (2.24)$$

The matrix \mathbf{D} is the Jacobian of the transformation from the $N+1$ final pseudo action variables to the $N+1$ initial variables.

Miller and Smith³⁷ and Hubbard and Miller^{38,39} then used first order classical perturbation theory, in which the small parameters are the corrugation height h and the coupling parameters c_j , $j = 1, \dots, N$ for the bath variables, setting the Jacobian prefactor to unity, to derive a relatively simple expression for the transition probability in terms of integer Bessel functions,

$$|S_{n, n_f; 0, n_i}|^2 = J_n^2(hA(\omega_x)) \prod_{j=1}^N J_{n_{j_f} - n_{j_i}}^2(\bar{A}_j(n_{j_{if}})), \quad (2.25)$$

with

$$n_{j_{if}} = \frac{n_{j_i} + n_{j_f}}{2}. \quad (2.26)$$

The arguments of the Bessel functions for the bath variables are

$$\bar{A}_j(n) = c_j \sqrt{\frac{2\hbar(n + \frac{1}{2})}{M\omega_j}} A(\omega_j), \quad (2.27)$$

with

$$A(\omega) = \frac{1}{\hbar} \int_{-\infty}^{+\infty} dt \bar{V}'(z_{t,0}) \cos \omega t. \quad (2.28)$$

Here, $z_{t,0}$ is the zero-th order solution for the classical vertical motion governed by

$$M\ddot{z}_{t,0} + \bar{V}'(z_{t,0}) = 0, \quad (2.29)$$

with the initial condition that the vertical momentum is p_{z_i} and the initial coordinate z_i is sufficiently far out such that the potential $\bar{V}(z_i)$ vanishes.

C. Thermal averaging

All that remains to be done is to perform the summation over final bath states and averaging over initial bath states to

obtain the final momentum distribution and the related angular distribution. For this purpose, using the notation

$$\tan \theta(n) = \frac{2\pi\hbar n}{l|p_{z_i}|}, \quad (2.30)$$

we note that energy conservation (Eq. (2.6)) implies that the final vertical momentum is a function of the initial vertical momentum, the Bragg quantum number, and the initial and final horizontal and bath actions,

$$p_{z_{t_0}}^2 = |p_{z_i}|^2 \left[\frac{\cos(|\theta_i| + 2\theta(n))}{\cos|\theta_i| \cos^2\theta(n)} - \frac{2M\hbar\Delta\mathbf{n} \cdot \boldsymbol{\omega}}{|p_{z_i}|^2} \right] \equiv |p_{z_i}|^2 \zeta(n, \Delta\mathbf{n} \cdot \boldsymbol{\omega})^2 \quad (2.31)$$

and energy conservation imposes the condition that

$$\zeta(n, \Delta\mathbf{n} \cdot \boldsymbol{\omega}) \geq 0. \quad (2.32)$$

Inserting unity as $1 = \int_{-\infty}^{\infty} d\bar{\Omega} \delta(\bar{\Omega} - \Delta\mathbf{n} \cdot \boldsymbol{\omega})$ and then using the Fourier representation of the Dirac delta function imply that the thermally averaged final momentum distribution may be rewritten as (with $H(x)$ denoting the unit step function)

$$\langle P(p_{x_f}, p_{z_f}) \rangle_{\beta} = \sum_n \int_{-\infty}^{\infty} d\bar{\Omega} \delta(p_{x_f} - p_{x_i} - \frac{2\pi\hbar n}{l}) \times \delta(p_{z_f} - |p_{z_i}| \zeta(n, \bar{\Omega})) H(\zeta(n, \bar{\Omega})) \times \tilde{F}(\bar{\Omega}, \beta, n). \quad (2.33)$$

All the dynamical information is hidden within the “form factor” $F(\tau, \beta, n)$ defined as

$$F(\tau, \beta, n) = \frac{1}{Z_B} \sum_{n_i=0}^{\infty} \sum_{n_f=0}^{\infty} P_{n, n_f; 0, n_i} \exp \left[-i\tau \Delta\mathbf{n} \cdot \boldsymbol{\omega} - \beta\hbar \left(\left(\mathbf{n}_i + \frac{1}{2} \mathbf{I} \right) \cdot \boldsymbol{\omega} \right) \right], \quad (2.34)$$

with

$$\tilde{F}(\bar{\Omega}, \beta, n) = \frac{1}{2\pi} \int_{-\infty}^{\infty} d\tau \exp(i\tau \bar{\Omega}) F(\tau, \beta, n). \quad (2.35)$$

The associated angular distribution is

$$\langle P(\theta_f) \rangle_{\beta} = \sum_n \int_{-\infty}^{\infty} d\bar{\Omega} \delta \left(\theta_f - \tan^{-1} \left(\frac{p_{x_i} + \frac{2\pi\hbar n}{l}}{|p_{z_i}| \zeta(n, \bar{\Omega})} \right) \right) \times H(\zeta(n, \bar{\Omega})) \tilde{F}(\bar{\Omega}, \beta, n). \quad (2.36)$$

This may be rewritten in the more convenient form

$$\langle P(\theta_f) \rangle_{\beta} = \sum_n \frac{2E_i \sin^2(|\theta_i| + \theta(n))}{\hbar \cos^2\theta(n) \sin^2\theta_f \tan\theta_f} \cdot \int_{-\infty}^{\infty} d\bar{\Omega} \delta \left(\bar{\Omega} - \frac{E_i}{\hbar} \left[1 - \frac{\sin^2(|\theta_i| + \theta(n))}{\sin^2\theta_f \cos^2\theta(n)} \right] \right) \times H(\zeta(n, \bar{\Omega})) \tilde{F}(\bar{\Omega}, \beta, n), \quad (2.37)$$

with

$$E_i = \frac{p_{x_i}^2 + p_{z_i}^2}{2M}. \quad (2.38)$$

Equations (2.32) and (2.37) are exact. However, within the semiclassical perturbation theory, the transition probability

factorizes so that one may rewrite the form factor in terms of a product of separate form factors for each oscillator,

$$F(\tau, \beta, n) = J_n^2(hA(\omega_x)) \prod_{j=1}^N f_j(\tau, \beta), \quad (2.39)$$

with

$$f_j(\tau, \beta) = [1 - \exp(-\hbar\beta\omega_j)] \sum_{n_f=0}^{\infty} \sum_{n_i=0}^{\infty} \exp[-n_i\hbar\beta\omega_j - i\tau\omega_j(n_f - n_i)] J_{n_f-n_i}^2(\bar{A}_j(n_{jif})). \quad (2.40)$$

Equations (2.39) and (2.40) are central to the numerical computations which will be presented below. However, first, we consider their simplification resulting from the fact that the coupling to the bath modes is weak.

Keeping in mind that the argument of the Bessel functions $\bar{A}_j(n_{jif})$ is linear in the coupling coefficients c_j and thus small, one may expand to first order in c_j^2 . This implies that only no phonon or single phonon transitions ($\Delta n = 0, \pm 1$) contribute to the j -th form factor,

$$f_j(\tau, \beta, \Delta n = 0) \simeq 1 - \frac{c_j^2 A^2(\omega_j)}{2M\omega_j} \hbar \coth\left(\frac{\hbar\beta\omega_j}{2}\right), \quad (2.41)$$

$$f_j(\tau, \beta, \Delta n = 1) \simeq \exp(-i\tau\omega_j) \times \frac{\hbar c_j^2 A^2(\omega_j)}{2M\omega_j [1 - \exp(-\hbar\beta\omega_j)]}, \quad (2.42)$$

$$f_j(\tau, \beta, \Delta n = -1) \simeq \exp(i\tau\omega_j) \times \frac{\hbar c_j^2 A^2(\omega_j) \exp(-\hbar\beta\omega_j)}{2M\omega_j [1 - \exp(-\hbar\beta\omega_j)]}. \quad (2.43)$$

Allowing then only up to a change of one phonon during the collision process implies that

$$F(\tau, \beta, n) \simeq J_n^2(hA(\omega_x)) \prod_{j=1}^N f_j(\tau, \beta, \Delta n = 0) \times \left[1 + \sum_{j=1}^N \frac{f_j(\tau, \beta, \Delta n = 1) + f_j(\tau, \beta, \Delta n = -1)}{f_j(\tau, \beta, \Delta n = 0)} \right]. \quad (2.44)$$

Using the definition of the spectral density (Eq. (2.3)) and the exponentiation $1 - x \simeq \exp(-x)$, one readily finds that

$$\prod_{j=1}^N f_j(\tau, \beta, \Delta n = 0) = \exp(-2W), \quad (2.45)$$

and the Debye Waller factor is

$$W = \frac{1}{2\pi\hbar M} \int_{-\infty}^{+\infty} dt_1 \int_{-\infty}^{+\infty} dt_2 \bar{V}'(z_{t_1,0}) \bar{V}'(z_{t_2,0}) \times \int_0^{\infty} d\omega J_z(\omega) \cos[\omega(t_1 - t_2)] \coth\left(\frac{\hbar\beta\omega}{2}\right). \quad (2.46)$$

The same expression has been derived previously for neutron scattering through surfaces in Ref. 46 and for surface scattering in Ref. 47.

The single phonon contributions may also be written in the continuum limit. Defining

$$F_1(\tau, \beta) \equiv \sum_{j=1}^N \frac{f_j(\tau, \beta, \Delta n = 1) + f_j(\tau, \beta, \Delta n = -1)}{f_j(\tau, \beta, \Delta n = 0)}, \quad (2.47)$$

one may readily carry out the Fourier transform over τ in Eq. (2.33) and using the definition of the spectral density to find that

$$\begin{aligned} \tilde{F}_1(\bar{\Omega}, \beta) &\equiv \frac{1}{2\pi} \int_{-\infty}^{\infty} d\tau \exp(i\tau\bar{\Omega}) F_1(\tau, \beta) \\ &= \frac{J_z(|\bar{\Omega}|) [H(\bar{\Omega}) + H(-\bar{\Omega}) \exp(-\hbar\beta|\bar{\Omega}|)]}{\pi\hbar M [1 - \exp(-\hbar\beta|\bar{\Omega}|)]} \\ &\quad \cdot \int_{-\infty}^{+\infty} dt_1 \int_{-\infty}^{+\infty} dt_2 \bar{V}'(z_{t_1,0}) \bar{V}'(z_{t_2,0}) \cos[\bar{\Omega}(t_1 - t_2)]. \end{aligned} \quad (2.48)$$

One then finds that the resulting final angular distribution is

$$\begin{aligned} \langle P(\theta_f) \rangle_{\beta} &= \exp(-2W) \sum_n \frac{\sin(|\theta_i| + \theta(n))}{\sin\theta_f \cos\theta(n)} J_n^2(hA(\omega_x)) \cdot \delta\left[\theta_f - \sin^{-1}\left(\frac{\sin(|\theta_i| + \theta(n))}{\cos\theta(n)}\right)\right] H(\zeta(n, 0)) \\ &\quad + \exp(-2W) \sum_n \frac{2J_n^2(hA(\omega_x))}{\tan\theta_f} \cdot \int_{-\infty}^{\infty} d\bar{\Omega} \left(\frac{E_i}{\hbar} - \bar{\Omega}\right) \delta\left(\frac{E_i}{\hbar} - \bar{\Omega} - \frac{E_i \sin^2(|\theta_i| + \theta(n))}{\hbar \sin^2\theta_f \cos^2\theta(n)}\right) H(\zeta(n, \bar{\Omega})) \tilde{F}_1(\bar{\Omega}, \beta, n). \end{aligned} \quad (2.49)$$

The zero phonon contribution is thus a series of delta function peaks at the Bragg angles whose intensity is temperature dependent, via the Debye-Waller factor. The single phonon transitions contribute a smooth background to the angular

distribution, since the function $\tilde{F}_1(\bar{\Omega}, \beta, n)$ is a smooth function of the phonon frequency $\bar{\Omega}$. One may continue this process to also include the two phonon contribution, the explicit expression may be found in Eqs. (15)-(18) of Ref. 42.

III. IMPLEMENTATION TO SCATTERING OF Ne, Ar, AND Kr ON Cu(111)

A. Theoretical considerations

A central purpose of this paper is to compute the thermal angular distribution within the semiclassical perturbation theory framework but without restricting the theory to only a few phonon transitions. To achieve this, we discretize the problem, that is, instead of using continuum limit expressions, we assume a continuum limit spectral density and then approximate it with a finite sum over harmonic oscillators. Then for each oscillator, we compute its form factor as given in Eq. (2.40).

The discretization is carried out following the methodology of Refs. 48 and 49 (for different discretizations, see Refs. 50 and 51). The spectral density is modeled as Ohmic with an exponential cutoff, that is,

$$J_z(\omega) = \gamma\omega \exp\left(-\frac{\omega}{\omega_c}\right), \quad (3.1)$$

γ is the friction coefficient and ω_c is referred to as the cutoff frequency, although, in fact, it is the frequency at which the spectral density reaches its maximum value.

To evaluate the angular distribution, the bath oscillator frequencies ω_j and coupling coefficients c_j are needed. Following the suggestion of Ref. 48 for $N_B + 1$ bath oscillators, the discretized frequencies for the first N_B oscillators are determined as

$$\omega_j = -\omega_c \ln\left(1 - \frac{j}{N_B + 1}\right), \quad j = 1, \dots, N_B \quad (3.2)$$

and the associated coupling coefficients as

$$c_j = \sqrt{\frac{2\omega_j^2 \gamma \omega_c}{\pi(N_B + 1)}}, \quad j = 1, \dots, N_B. \quad (3.3)$$

The Fourier transform of the form factor is computed by introducing a Gaussian smoothing,

$$\langle \tilde{F}(\bar{\Omega}, \beta, n) \rangle = \frac{1}{2\pi\sqrt{2\pi T_{sm}^2}} \int_{-\infty}^{\infty} d\tau \times \exp\left(-\frac{\tau^2}{2T_{sm}^2} + i\tau\bar{\Omega}\right) F(\tau, \beta, n). \quad (3.4)$$

The smoothing period T_{sm} is chosen to be

$$T_{sm} = \frac{2\pi}{\Delta\omega}, \quad (3.5)$$

where $\Delta\omega$ is taken to be a typical spacing between adjacent frequencies of the discretized oscillators.

B. The Morse potential model

To apply the theory, we choose the vertical interaction potential to be the Morse potential

$$\tilde{V}(z) = V_0[(\exp(-\alpha z) - 1)^2 - 1], \quad (3.6)$$

which is characterized by the well depth V_0 and the stiffness parameter α . The advantage of the Morse form is that the arguments of the Bessel functions may be evaluated analytically.

TABLE I. Parameters used for Ne, Ar, and Kr atoms scattered on a Cu(111) surface.

Atom	αl	V_0 (meV)	$\bar{\gamma}$	h (a.u.)
Kr	4.2	134.0	0.120 5	2.82×10^{-3}
Ar	3.3	70.0	0.057 82	1.98×10^{-3}
Ne	3.0	31.6	0.012 34	1.10×10^{-3}

One readily finds (Ref. 32) that (see Eq. (2.28))

$$A(\omega) = -\frac{2\pi M\omega}{\alpha\hbar} \frac{\cosh(\Phi\frac{\omega}{\Omega})}{\sinh(\pi\frac{\omega}{\Omega})}, \quad (3.7)$$

with

$$\Omega^2 = \frac{2\alpha^2 E_z}{M} \quad (3.8)$$

and

$$\cos(\Phi) = -\sqrt{\frac{V_0}{E_z + V_0}}. \quad (3.9)$$

C. Application to scattering of Ne, Ar, and Kr from Cu(111)

The SCPT theory is now applied to analyze and interpret the measured low temperature angular distribution of Ne, Ar, and Kr atoms scattered from a Cu(111) surface.^{40,41} The parameters used (Table I) are the same as in Ref. 42. The well depths of the Morse potentials for all three cases were taken from recent *ab-initio* computations.⁵² The lattice length is 3.61 Å.⁵³ The corrugation height was determined from the measured ratio of the $n = 0$ to $n = -1$ Bragg peaks since this ratio determines the magnitude of the phase amplitude $hA(\omega_x)$ appearing in the argument of the respective Bessel functions.

The spectral density is chosen to be Ohmic (for a theoretical justification, see Ref. 54) with an exponential cutoff $J(\omega) = \gamma\omega \exp(-\omega/\omega_c)$. The cutoff frequency, $\hbar\omega_c = 6$ meV, is the same for all atoms since it is a property of the surface. It was chosen by fitting the Debye-Waller factor to the experimental data. The reduced friction coefficient ($\bar{\gamma} = M^2\omega_0^3\gamma$, where $\omega_0^2 = 2V_0\alpha^2/M$) is fit separately for each atom. The theory thus involves three parameters for each atom (γ, V_0, α) and the cutoff frequency ω_c , common to all cases. In all cases that will be presented using this model, the elastic peaks were Gaussian broadened ($\Delta\theta = 0.4^\circ$), to agree with the experimental broadening in the incident beam, as also detailed in Ref. 41.

A first check on the theory is to determine how well the continuum limit expression for the Debye-Waller factor (Eq. (2.46)) (obtained by expansion of the Bessel functions to lowest order and exponentiation) agrees with its discretized form which is a sum of the logarithm of the form factors as given in Eq. (2.45). The results are presented in Fig. 1. The good comparison between the continuum limit expression and the experimentally measured Debye-Waller factors has already been presented in Fig. 1 of Ref. 42 but is also added here (solid dots).

A second check of the present theory is to compare the results for the discretized theory (dashed lines) with the

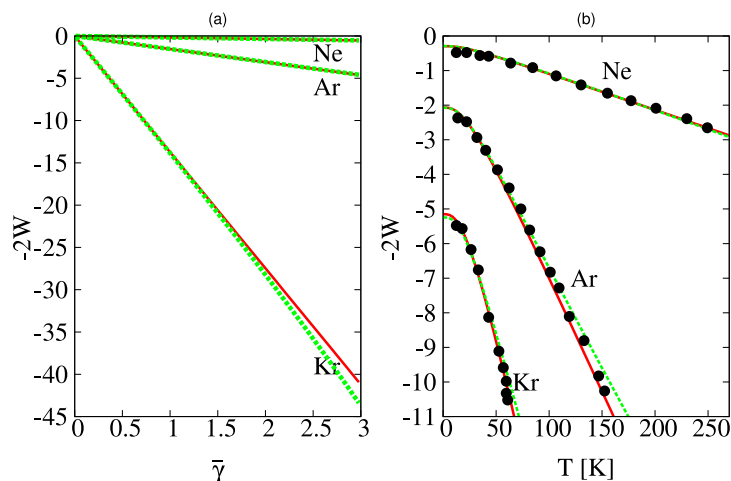


FIG. 1. Comparison of the continuum limit expression for the Debye-Waller factor (Eq. (2.46)) and its estimate as the discretized sum of the logarithm of the form factors (Eq. (2.45)). The results are presented (continuum limit — dashed, green line and discretized expression — solid, red line) for the scattering of Ne, Ar, and Kr as a function of the reduced friction coefficient in panel (a) and as a function of the surface temperature in panel (b). The solid dots are the experimental data of Ref. 41. The number of oscillators used was 40.

continuum limit expressions (solid lines) for up to two phonon contributions, as given in Eqs. (14)–(18) of Ref. 42. This is shown in Fig. 2. One notes that apart from the oscillations due to the finite discretization, there is good agreement between the various computations.

In Ref. 42, only up to two phonon contributions were included, using the continuum form. The comparison with the experimental results showed good agreement at very low temperature, but as the temperature was increased, especially for Ar and Kr scattering, there were deviations which we attributed to higher order phonon scattering contributions. That this is so is evident from Fig. 3 where we plot the angular distributions obtained using one-, two-, and multi-phonon contributions. As the temperature is increased, the all phonon contribution becomes larger relative to the continuum one and two phonon results.

Finally, in Fig. 4, we compare the discretized theory, including all multi-phonon contributions with the experimental results of Ref. 41. We find good agreement between experiment and theory for the scattering of Ne and Ar (the small

oscillations in the theoretical results are due to the finite number of oscillators used, increasing the number reduces the oscillations). From Fig. 3, it is clear that for Ne, more than two phonon transitions are not important, even at room temperature. This is not the case for the scattering of Ar, where only inclusion of the multi-phonon transitions at $T = 84$ K gives quantitative agreement with experiment. Finally, for Kr scattering, the results, especially at the higher temperature ($T = 42$ K) where the multi-phonon contributions are significant, are in better agreement with experiment than the previous results based on only up to two phonon transitions. We do note that already the low temperature theoretical results, presented in Ref. 42, were a bit low, so the lack of quantitative agreement is not surprising.

IV. DISCUSSION

In this paper, we derived a new semiclassical multi-phonon theory for atom surface scattering. Using a discretized

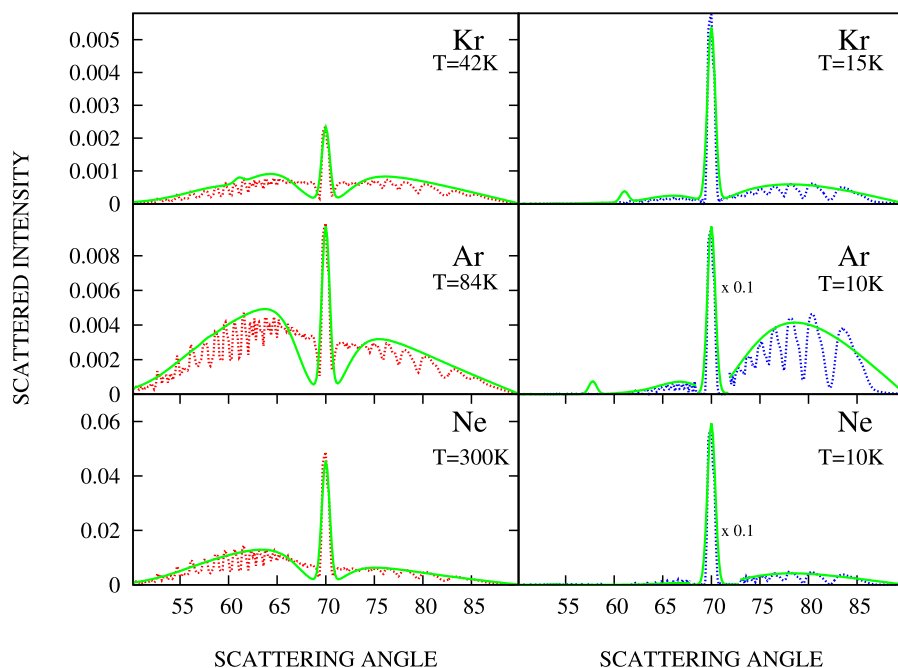


FIG. 2. Comparison between the discretized theory (dotted red and blue lines) and the continuum (solid green lines) angular distributions when only one and two phonon contributions are allowed. Apart from the oscillatory character of the discretized results, there is good agreement between the two computations. The number of oscillators used for the discretization was 20.

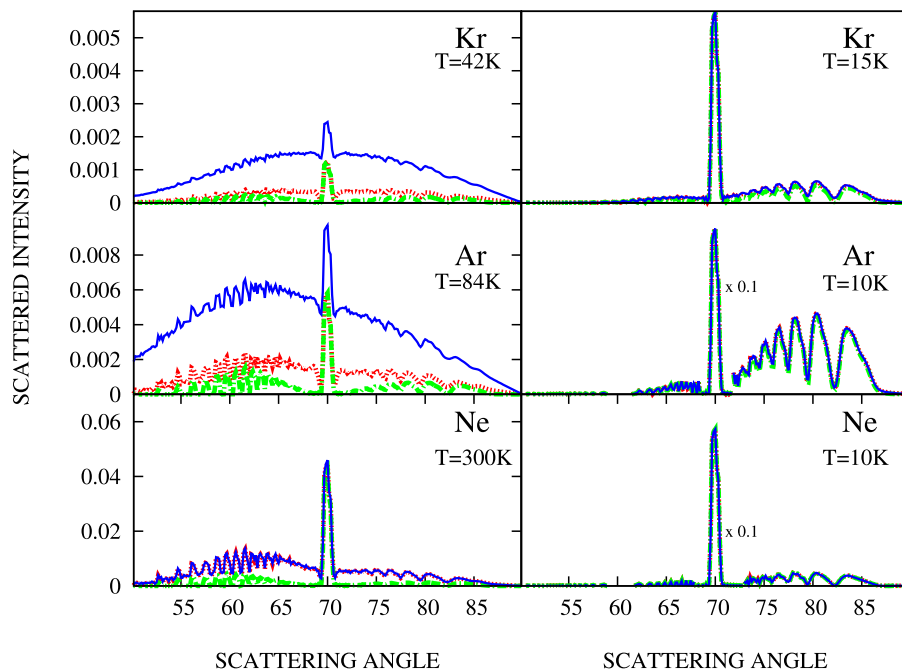


FIG. 3. The contributions of multi-phonon transitions as the surface temperature is increased. The one (dashed-dotted green lines), one + two (dotted red lines) and all phonon (solid blue lines) contributions are shown for the angular distributions of Ne, Ar, and Kr, scattered on the Cu(100) surface. Note the increased contribution from multi-phonon transitions as the temperature is increased. The number of oscillators used in the discretized computation is 20.

representation of the spectral density, an expression was derived for the angular distribution for an atom scattered from a thermal surface. The discretized results were shown to be in good agreement with the continuum results, both for the Debye-Waller factor as well as for low temperature scattering when only up to two phonon transitions are important. The multi-phonon theory accounts well for the measured features of the angular distribution, which are the superposition of elastic “delta” function peaks on a smooth and broad background whose intensity increases as the surface temperature is increased.

The multi-phonon theory confirms our previous conjecture given in Ref. 42 that the broad background measured in the angular distribution at increased surface temperature comes

from multi-phonon transitions. Comparison of the present theory with the experimentally measured results was favorable; we note that we used the same parameters as in our previous Communication.⁴²

The theory presented here can be developed in further directions. One is a study of the energy transferred from the scattered atom to and from the bath, as a function of angle of incidence, incident energy, and surface temperature. A second direction is extension to include second order surface corrugation effects.⁵⁵ It should also be possible to extend the present formulation of a multi-phonon theory based on the definition of a form factor to the continuum limit. Finally, the theory should be readily applicable to many experimental results on atom surface scattering.

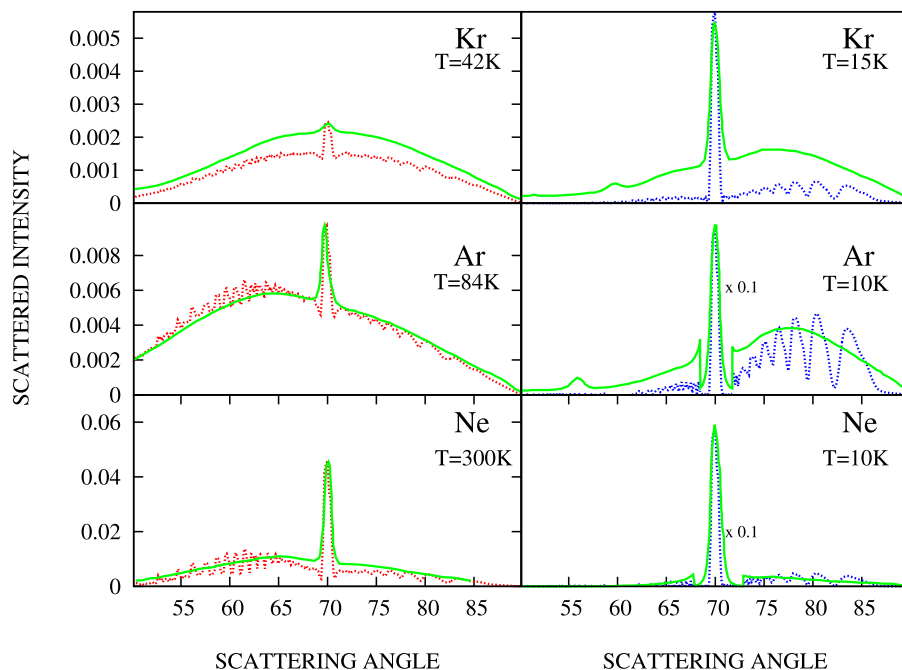


FIG. 4. Comparison of the theoretically generated (dashed red and blue lines) angular distributions using the multi-phonon discretized theory with the experimental measurements (solid green lines) of Ref. 41 for the scattering of Ne, Ar, and Kr on the Cu(100) surface. The experimental and theoretical distributions were scaled to agree with each other at the specular peak. The discretized theory is based on 20 oscillators.

ACKNOWLEDGMENTS

We thank Professor S. Miret-Artés for stimulating discussion. This work was supported by grants from the Israel Science Foundation, the German Israel Foundation for Basic Research and the Minerva Foundation (Munich).

- ¹F. Knauer and O. Stern, *Z. Phys.* **53**, 779 (1929).
- ²I. Estermann and O. Stern, *Z. Phys.* **61**, 95 (1930).
- ³G. Benedek and J. P. Toennies, *Surf. Sci.* **299-300**, 587 (1994).
- ⁴N. Cabrera, V. Celli, F. O. Goodman, and R. Manson, *Surf. Sci.* **19**, 67 (1970).
- ⁵N. Cabrera, V. Celli, and R. Manson, *Phys. Rev. Lett.* **22**, 346 (1969).
- ⁶J. R. Manson, *Phys. Rev. B* **43**, 6924 (1991).
- ⁷G. D. Billing, *Chem. Phys.* **70**, 223 (1982).
- ⁸G. D. Billing, *Chem. Phys.* **74**, 143 (1983).
- ⁹R. Guantesa, A. S. Sanz, J. Margalef-Roiga, and S. Miret-Artés, *Surf. Sci. Rep.* **53**, 199 (2004).
- ¹⁰A. S. Sanz and S. Miret-Artés, *Phys. Rep.* **451**, 37 (2007).
- ¹¹R. Martínez-Casado, S. Miret-Artés, B. Meyer, F. Traeger, and C. Woll, *J. Phys.: Condens. Matter* **22**, 304011 (2010).
- ¹²M. Mayrhofer-Reinhartshuber, P. Kraus, A. Tamtögl, S. Miret-Artés, and W. E. Ernst, *Phys. Rev. B* **88**, 205425 (2013).
- ¹³P. Kraus, M. Mayrhofer-Reinhartshuber, C. Gosweiner, F. Apolloner, S. Miret-Artés, and W. E. Ernst, *Surf. Sci.* **630**, 208-215 (2014).
- ¹⁴B. Jackson, *J. Chem. Phys.* **90**, 140 (1989); **92**, 1458 (1990).
- ¹⁵B. Jackson and H. Metiu, *J. Chem. Phys.* **86**, 1026 (1987).
- ¹⁶B. Gumhalter, *Phys. Rep.* **351**, 1 (2001).
- ¹⁷K. Burke, B. Gumhalter, and D. C. Langreth, *Phys. Rev. B* **47**, 12852 (1993).
- ¹⁸B. Gumhalter, K. Burke, and D. C. Langreth, *Surf. Rev. Lett.* **1**, 133 (1994).
- ¹⁹A. Gross, in *Handbook of Material Modeling*, edited by S. Yip (Springer, 2005), p. 1713.
- ²⁰A. Gross and M. Scheffler, *Chem. Phys. Lett.* **263**, 567 (1996).
- ²¹P. Nieto, E. Pijper, D. Barredo, G. Laurent, R. A. Olsen, E.-J. Baerends, G.-J. Kroes, and D. Faras, *Science* **312**, 86 (2006).
- ²²G. Drolshagen and E. J. Heller, *J. Chem. Phys.* **79**, 2072 (1983).
- ²³S. Miret-Artés and E. Pollak, *Surf. Sci. Rep.* **67**, 161 (2012).
- ²⁴R. M. Logan and R. E. Stickney, *J. Chem. Phys.* **44**, 195 (1966).
- ²⁵R. M. Logan and J. C. Keck, *J. Chem. Phys.* **49**, 860 (1968).
- ²⁶J. C. Tully, *J. Chem. Phys.* **92**, 680 (1990).
- ²⁷W. A. Steele, *Surf. Sci.* **38**, 1 (1973).
- ²⁸U. Garibaldi, A. C. Levi, R. Spadacini, and G. E. Tommei, *Surf. Sci.* **48**, 649 (1975).
- ²⁹E. F. Greene and E. A. Mason, *Surf. Sci.* **75**, 549 (1978).
- ³⁰J. R. Klein and M. W. Cole, *Surf. Sci.* **79**, 269 (1979).
- ³¹E. Pollak, S. Sengupta, and S. Miret-Artés, *J. Chem. Phys.* **129**, 054107 (2008).
- ³²E. Pollak, J. M. Moix, and S. Miret-Artés, *Phys. Rev. B* **80**, 165420 (2009); Erratum **81**, 039902 (2010).
- ³³E. Pollak and J. Tatchen, *Phys. Rev. B* **80**, 115404 (2009); Erratum **81**, 049903 (2010).
- ³⁴E. Pollak and S. Miret-Artés, *J. Chem. Phys.* **130**, 194710 (2009); Erratum **132**, 049901 (2010).
- ³⁵E. Pollak and S. Miret-Artés, *Chem. Phys.* **375**, 337 (2010).
- ³⁶Y. Zhou, E. Pollak, and S. Miret-Artés, *J. Chem. Phys.* **140**, 024709 (2014).
- ³⁷W. H. Miller and F. T. Smith, *Phys. Rev. A* **17**, 939 (1978).
- ³⁸L. M. Hubbard and W. H. Miller, *J. Chem. Phys.* **78**, 1801 (1983).
- ³⁹L. M. Hubbard and W. H. Miller, *J. Chem. Phys.* **80**, 5827 (1984).
- ⁴⁰F. Althoff, T. Andersson, and S. Andersson, *Phys. Rev. Lett.* **79**, 4429 (1997).
- ⁴¹T. Andersson, F. Althoff, P. Linde, S. Andersson, and K. Burke, *Phys. Rev. B* **65**, 045409 (2002).
- ⁴²S. Daon, E. Pollak, and S. Miret-Artés, *J. Chem. Phys.* **137**, 201103 (2012).
- ⁴³A. Azuri and E. Pollak, *J. Chem. Phys.* **139**, 044707 (2013).
- ⁴⁴W. H. Miller, *J. Chem. Phys.* **53**, 1949 (1970).
- ⁴⁵W. H. Miller, *J. Chem. Phys.* **53**, 3578 (1970).
- ⁴⁶Equation (2) of V. F. Sears and S. A. Shelley, *Acta Crystallogr., Sect. A: Found. Crystallogr.* **A47**, 441 (1991).
- ⁴⁷Equations (4.35) and (4.36) of A. C. Levi and H. Suhl, *Surf. Sci.* **88**, 221 (1979); K. Burke and W. Kohn, *Phys. Rev. B* **43**, 2477 (1991).
- ⁴⁸H. Wang, M. Thoss, and W. H. Miller, *J. Chem. Phys.* **112**, 47 (2000).
- ⁴⁹M. Thoss, H. Wang, and W. H. Miller, *J. Chem. Phys.* **114**, 9220 (2001).
- ⁵⁰C.-M. Goletz, W. Koch, and F. Grossmann, *Chem. Phys.* **375**, 227 (2010).
- ⁵¹N. Wu, L. Duan, X. Li, and Y. Zhao, *J. Chem. Phys.* **138**, 084111 (2013).
- ⁵²P. L. Silvestrelli, A. Ambrosetti, S. Grubisic, and F. Ancilotto, *Phys. Rev. B* **85**, 165405 (2012).
- ⁵³M. Wilms, P. Broekman, C. Stuhlmann, and K. Wandelt, *Surf. Sci.* **416**, 121 (1998).
- ⁵⁴Y. Georgievskii, M. A. Kozhushner, and E. Pollak, *J. Chem. Phys.* **102**, 6908 (1995).
- ⁵⁵E. Pollak and S. Miret-Artés, "Second-order semiclassical perturbation theory for diffractive scattering from a surface," *J. Phys. Chem. C* (published online).